*Transactions of the Materials Research Society of Japan* 29 [2] 599-602 (2004)

# Ion Implantation into ePTFE for Therapy of Broad-based Brain Aneurysms

Y. Ono[1,4], T.Tsukamoto[1], N. Takahashi[1], T. Yotoriyama[1], Y. Suzuki[2], M. Iwaki[2], H. Ujiie[3], and T. Hori[3]

[1]Tokyo University of Science, 1-3, Kagurazaka, Shinjuku-ku, Tokyo 162-8601 Japan
e-mail: yono@iem.titech.ac.jp
[2]Beam Application Team, RIKEN, Japan.
[3]Tokyo Women's Medical University, Japan.
[4]Tokyo Institute of Technology, Japan

Intracranial internal brain artery aneurysms are frequently treated by microsurgical clipping of the aneurysm neck (by endovascular coiling of the aneurysm sac), or by balloon occlusion of the parent vessel. For some broad-based aneurysms not suitable for these options, a rare microsurgical wrapping of the aneurysm wall with muslin or gauze is applied. Ion implantation was utilized to alter the surface properties (cell migration and adhesion) of expanded polytetrafluoroethyrene (ePTFE) wrapping material for treatment of brain aneurysms. Ion-implanted ePTFE sheets were applied as wrapping materials. We evaluated the effectiveness of this therapy on brain aneurysms for studying ion-implanted ePTFE on the wall of arteries. $Ar^+$ ($5\times10^{14}$ ions/cm$^2$) and $Kr^+$ ($1\times10^{14}$ ions/cm$^2$) ions were implanted into ePTFE at an energy of 150 keV. An in vitro and in vivo study demonstrated that ion-implanted ePTFE exhibits remarkably greater adhesion and spreading of living cells than non-implanted specimens. The internodal distance, density between the nodes, OH radical, and C=C bond induced by ion-implantation were the major factors that influenced cell invasion in ion-implanted ePTFE. The results of this investigation indicate that application of this technology would prevent rupture of aneurysms.

Key words: Cell attachment, Cell migration, Wrapping material, In vivo study

## 1. INTRODUCTION

Artificial organs, such as replacements of artificial dura matter, are steadily increasing in importance as replacements for body functions. Ion implantation has proven to be a useful technique for improving the surface properties of metals [1], and polymers [2]. In recent years, ion implantation has been used for the surface modification of polymers to improve blood compatibility [3],[4],[5], tissue compatibility [6], and the clinical application of this technique [7],[8].

The adhesion, growth, and proliferation of endothelial cells in cell culture are anchorage-dependent. It is supposed that the adhesion of endothelial cells is mainly influenced by the nature of the substrate. Many investigations have been introduced focusing on the development of biocompatible materials, and the improvement of cell attachment to such surfaces [9].

Every year twelve people per one hundred thousand die of subarachnoid hemorrhage from ruptured brain aneurysms. In this research, we implant ions into expanded polytetrafluoroethyrene (ePTFE) to produce cell adhesive materials to wrap brain aneurysms and prevent subarachnoid hemorrhage. An in vitro and in vivo study of ion-implanted ePTFE was performed using rabbits to develop cell adhesive artificial wrapping materials in relation to the ion species and surface characteristics.

## 2. MATERIALS AND METHODS

### 2.1 Ion Implantation

The specimens were ePTFE sheets (PSM-01200, W.L. Gore and Associates, United States). The structural formula is presented in Fig. 1. $Ar^+$ ($5\times10^{14}$ ions/cm$^2$) and $Kr^+$ ($1\times10^{14}$ ions/cm$^2$) ions were implanted into ePTFE at an energy of 150 keV at room temperature. The beam-current density was lower than 0.05 $\mu$ A/cm$^2$ to prevent temperature rising.

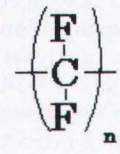


Fig. 1 Structural formula of ePTFE

### 2.2 In Vitro Cell Attachment Study

L929 fibroblasts cells were used for in vitro cell culture. This cell suspension was placed on the ion-implanted ePTFE in medium (RPMI1640; Nissui Pharmaceutical Co.) supplemented with

10% fetal bovine serum (FBS; Gibco Laboratories, Grand Island, NY). The initial number of cells seeded was $2.5 \times 10^4$ cells/ml. The cells were incubated for three days at 37℃ in 5% $CO_2$ in a humid atmosphere. The extent of cell attachment and spreading was determined visually with an optical microscope equipped with phase contrast objectives and a camera.

2.3 In Vivo Animal Study

Thirteen Japanese white rabbits weighing 3 to 4.5 kg were used in this study. Ion–implanted ePTFE was implanted subcutaneously on the carotid arteries after administering anesthesia of sodium pentobarbital. Non-implanted ePTFE and ion-implanted ePTFE were used for the test specimens. These specimens were wrapped around the rabbit's carotid arteries as depicted in Fig. 2. All the procedures were conducted under sterile conditions.

The animals were then killed by an intravenous overdose of KCl at different times, and the specimens were surgically removed for histopathological examination. The tissue was fixed in a 10% formalin solution, decalcified with formic acid, and stained with hematoxylin and eosin.

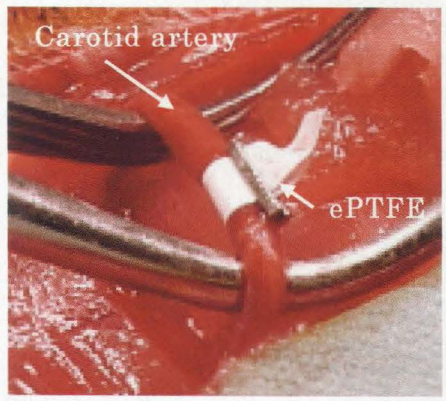


Fig. 2 In vivo tissue adhesive study

2.4 Physico-Chemical Properties

Ion-implanted and non-implanted ePTFE were coated with gold in a plasma coater (SG-701, Sanyu Denshi, Japan). Microphotographs of field emission scanning electron microscopy (SEM) were obtained at a 5 kV acceleration voltage (JED6330F, JEOL, Japan). Fourier transformed infrared spectroscopy analyses (in attenuated total reflectance mode, FT-IR-ATR) of $Ar^+$, $Kr^+$-implanted and non-implanted ePTFE surfaces were performed with an FT-IR-ATR spectrometer (NEXUS470, Nicolet, France). The analyses were conducted with an internal reflection element (Ge, 45° incident angle), 128 scans, and a resolution of 4 $cm^{-1}$.

## 3. RESULTS AND DISCUSSION

3.1 In Vitro Cell Attachment Study

Figure 3 illustrates fibroblast cell attachment to $5 \times 10^{14}$ ions/$cm^2$-$Ar^+$ (a) and $1 \times 10^{14}$ ions/$cm^2$-$Kr^+$ (b) ion-beam implanted circular domain with a diameter of 120 μm at 150 keV, after an incubation of 24 h. The seeded cells recognized the surface of ion-irradiated ePTFE and selectively attached to the ion-beam implanted domain. Cell attachment to the $Ar^+$ ion-implanted ePTFE domain further improved in performance as compared with $Kr^+$ ion-implanted ePTFE.

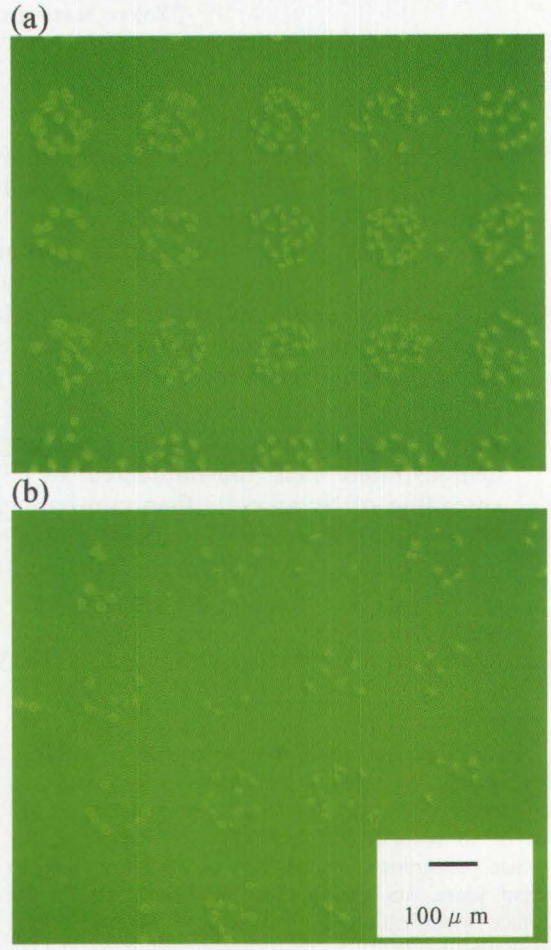


Fig. 3 Microphotographs of fibroblast cell attachment to $5 \times 10^{14}$ ions/$cm^2$-$Ar^+$ (a) and $1 \times 10^{14}$ ions/$cm^2$-$Kr^+$ (b) ion-implanted ePTFE ; 24 hours after incubation

3.2 In Vivo Animal Study

Figure 4 presents the histology of non-implanted (a), $Ar^+$ ion-implanted (b), and $Kr^+$ ion-implanted (c) ePTFE surfaces 30 days after implantation. There is no tissue integration along the entire non-implanted ePTFE surface. The circumvascular tissue contacting the ion-implanted ePTFE surface was composed of tissue in growth fibroblasts. A histological examination of the ion-implanted ePTFE after implantation exhibited excellent attachment in contact with the wall of the carotid artery. In addition, self-repair was observed. There was no significant difference between $Ar^+$ and $Kr^+$ ion-implanted ePTFE.

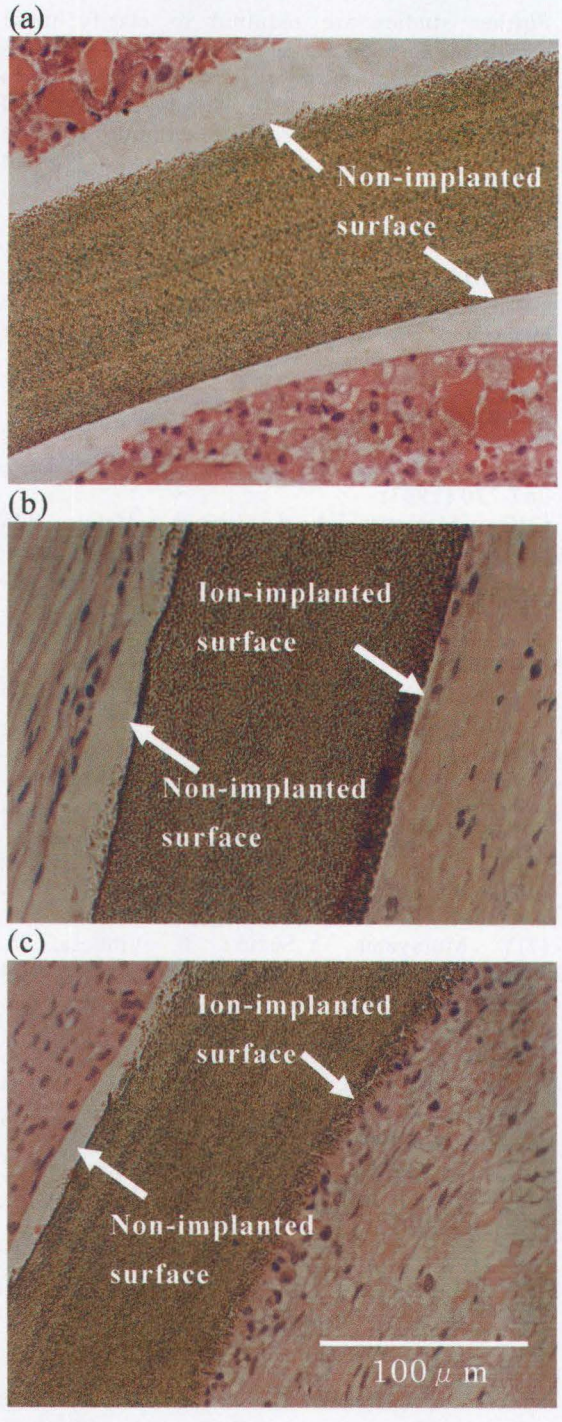


Fig.4 Photomicrographs of the tissue-material boundary surfaces of non-implanted (a), $Ar^+$ ($5\times10^{14}$ ions/cm$^2$) (b) and $Kr^+$ ($1\times10^{14}$ ions/cm$^2$)-implanted ePTFE; a week after implantation.

### 3.3 SEM Observations

The SEM micrographs of non-implanted (a), $Ar^+$ ion-implanted (b), and $Kr^+$ ion implanted ePTFE (c) were displayed in Fig. 5. As Fig. 5(a) indicates, the non-ion implanted ePTFE surface is comprised of evenly distributed pores and nodes. Figures 5(b) and (c) reveal obvious changes for $Ar^+$ and $Kr^+$ ion-implanted ePTFE; the nodes began to dent and porosity was increased. The morphology of $Ar^+$ ion-implanted ePTFE was changed largely in comparison with $Kr^+$ ion-implanted ePTFE.

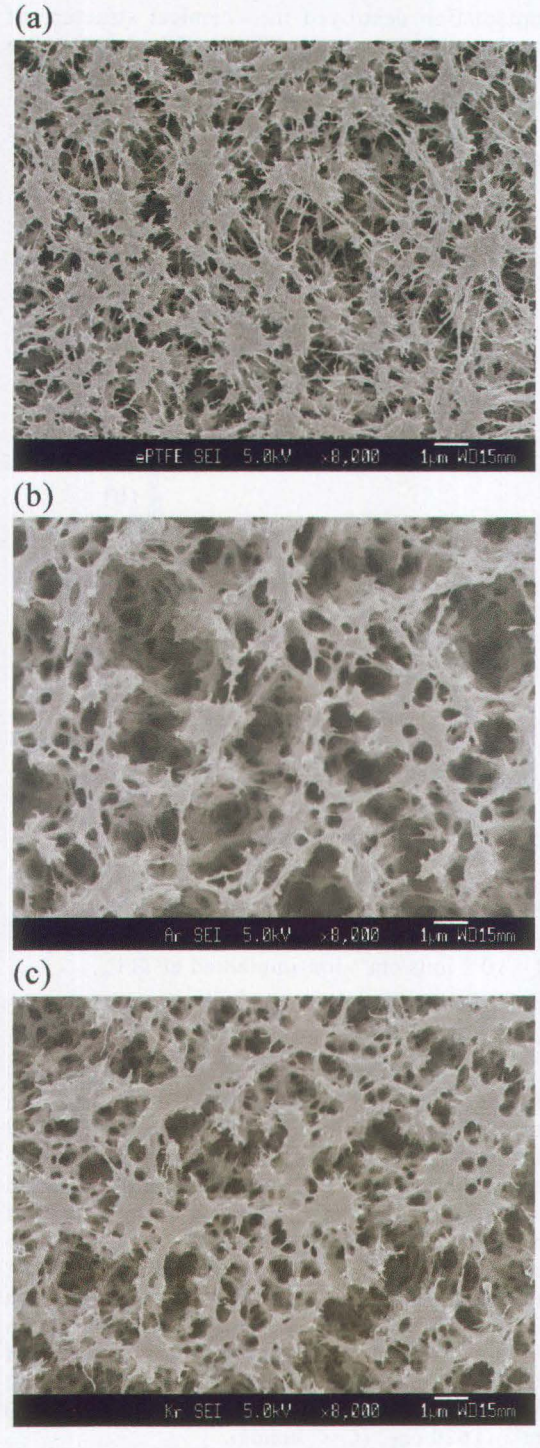


Fig. 5 SEM micrographs of (a) non-implanted, (b) $Ar^+$ ($5\times10^{14}$ ions/cm$^2$), and (c) $Kr^+$ ($1\times10^{14}$ ions/cm$^2$) ion-implanted ePTFE.

### 3.4. FT- IR- ATR study

The surface of ion-implanted ePTFE was

analyzed by FT-IR-ATR to study new functional groups and bond scission. Figure 6 illustrates the IR spectra of non-implanted(a), $Ar^+$ ion-implanted (b), and $Kr^+$ ion-implanted(c) ePTFE. FT-IR-ATR study indicates that ion implantation destroyed the chemical structure of the surface layer of ePTFE ($CF_2$ band). We observed the main characteristic band of ion-implanted ePFTE at 1680 $cm^{-1}$ - 1620 $cm^{-1}$ (C=C bonds). There was no significant difference between $Ar^+$ and $Kr^+$ ion-implanted ePTFE.

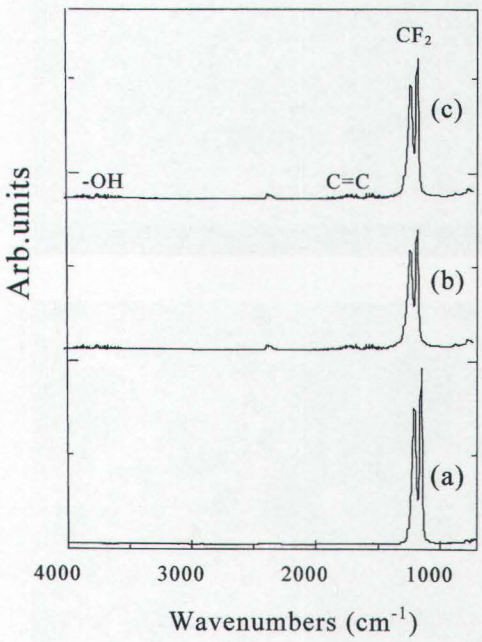


Fig. 6 FT-IR-ATR spectra of (a) non-implanted, (b) $Ar^+$ ($5\times10^{14}$ ions/$cm^2$) ion-implanted, and (c) $Kr^+$ ($1\times10^{14}$ ions/$cm^2$) ion-implanted ePTFE.

## 4. CONCLUSIONS

In vitro cell attachment to $Ar^+$ ion-implanted ePTFE domain demonstrated improved performance compared with $Kr^+$ ion-implanted ePTFE. A histological examination of the ion-implanted ePTFE after implantation revealed excellent attachment in contact with wall of carotid artery. The morphology was changed to largely that of $Ar^+$ ion-implanted ePTFE compared with $Kr^+$ ion-implanted ePTFE. An FT-IR-ATR study indicates that ion implantation destroyed the surface layer chemical structure of ePTFE ($CF_2$ band). The main characteristic band of ion-implanted ePFTE was observed at 1680 $cm^{-1}$ - 1620 $cm^{-1}$ (C=C bonds).

With ion-implanted ePTFE, internodal distance, density between the nodes, and C=C radical induced by ion-implantation were major factors influencing cell invasion. However, one possible explanation for the attachment of cells to the ion-implanted ePTFE could be the preferential adhesion of cell adhesive proteins from the surrounding tissue to the ion-implanted surface. Further studies are required to clarify these effects in more detail.

The implantation of ions into ePTFE surfaces is a promising approach for developing artificial wrapping materials to prevent the rupture of brain aneurysms. Therefore, it is very likely that ion-implanted ePTFE is applicable for clinical use.

ACKNOWLEDGMENT

This work was partly supported by an Open Research Grant from The Japan Research Promotion Society for Cardiovascular Diseases.

RERERENCES

[1]P. Sioshansi, *Nucl Insrum Meth* B, **24-5**, 767-770 (1987).
[2]G. Marletta. *Nucl Insrum Meth*, **B46 (1-4)**,295-305 (1990).
[3]Y. Suzuki, M. Kusakabe, H. Akiba, K. Kusakabe, and M. Iwaki. *Nucl Instrum Meth B*, **B59/60**, 698-704 (1991).
[4]Y. Suzuki, H. Iwata, A. Nakao, M. Iwaki, M. Kaibara, H. Sasabe, S. Kaneko, H. Nakajima, and M. Kusakabe. *Nucl Instrum Meth B*, **127**, 1019-1022 (1997).
[5]K. Kurotobi, M. Kaibara, Y. Suzuki, M. Iwaki, and H. Nakajima. *Nucl Instrum Meth B*, **B175**, 791-796 (2001).
[6]Y. Suzuki, M. Kusakabe, J-S Lee, M. Kaibara, M. Iwaki, and H. Sasabe. *Nucl Instrum Meth B*, **B65**, 142-147 (1992).
[7]Y. Murayama, Y.Suzuki, F. Vinuela, M. Kaibara, K. Kurotobi, M. Iwaki, and T. Abe. Part I: In vitro study. *Am J Neuroradiol*, **20**, 1986-1991 (1999).
[8]Y. Murayama, F. Vinuela, Y. Suzuki, Y. Akiba, A. Ulihoa, G. Duckwiler, Y. Gobin, H. Vinters, M. Iwaki,and T. Abe T. *Am J Neuroradiol*, **20**, 1992-1999 (1999).
[9]M. Kaibara, H. Iwata, H. Wada, Y. Kawamoto, M. Iwaki, and Y. Suzuki. *J Biomed Mat Res*, **31**, 429-435 (1996).

(Received October 9, 2003; Accepted January 20, 2004)